Accepted Manuscript

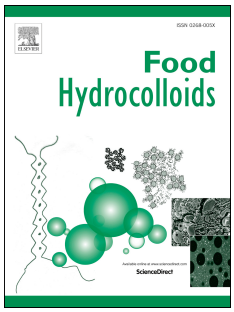

Comprehensive characterization of active chitosan-gelatin blend films enriched with different essential oils

Hossein Haghighi, Syméon Biard, Francesco Bigi, Riccardo De Leo, Elisa Bedin, Frank Pfeifer, Heinz Wilhelm Siesler, Fabio Licciardello, Andrea Pulvirenti

PII: S0268-005X(19)30442-4

DOI: https://doi.org/10.1016/j.foodhyd.2019.04.019

Reference: FOOHYD 5048

To appear in: *Food Hydrocolloids*

Received Date: 26 February 2019

Revised Date: 4 April 2019

Accepted Date: 10 April 2019

Please cite this article as: Haghighi, H., Biard, Symé., Bigi, F., De Leo, R., Bedin, E., Pfeifer, F., Siesler, H.W., Licciardello, F., Pulvirenti, A., Comprehensive characterization of active chitosan-gelatin blend films enriched with different essential oils, *Food Hydrocolloids* (2019), doi: https://doi.org/10.1016/j.foodhyd.2019.04.019.

Chitosan

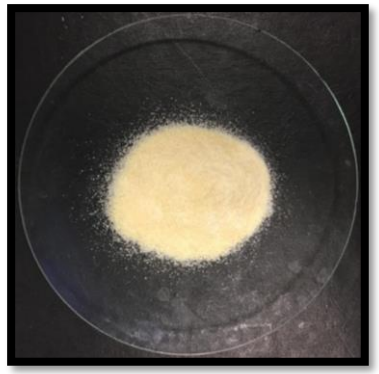

Gelatin

Chitosan-Gelatin Blend FFS

Essential oil (EO)

Chitosan-Gelatin-EO FFS

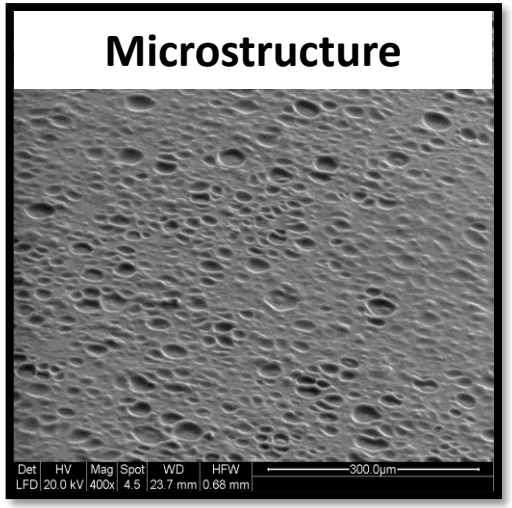

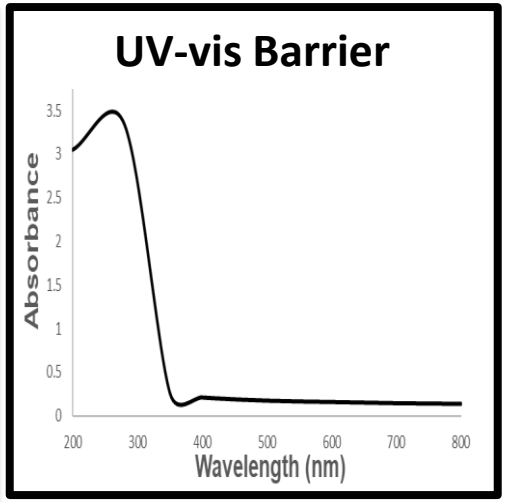

Food Packaging Applications

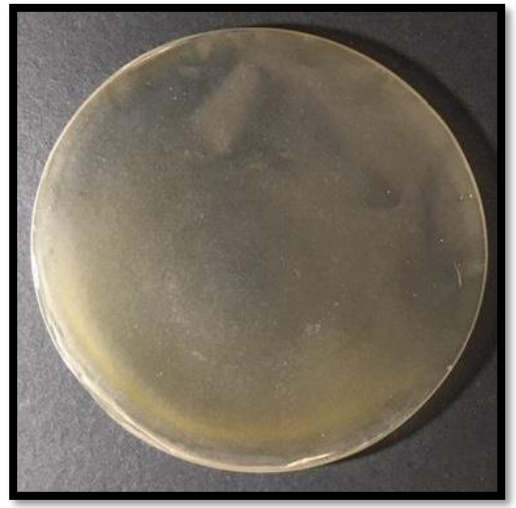

Chitosan-Gelatin-EO Film

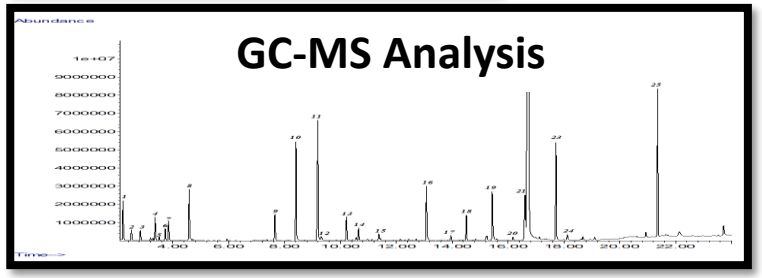

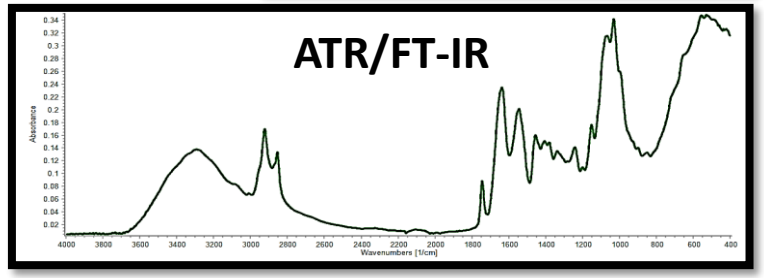

Comprehensive characterization of active chitosan-gelatin blend films enriched with different essential oils

Hossein Haghighi[a,*], Syméon Biard[b], Francesco Bigi[a], Riccardo De Leo[a], Elisa Bedin[a], Frank Pfeifer[c], Heinz Wilhelm Siesler[c], Fabio Licciardello[a,d], Andrea Pulvirenti[a,d]

[a] Department of Life Sciences, University of Modena and Reggio Emilia, 42122, Reggio Emilia, Italy

[b] Department of Agri-food, University of Caen Normandy, 14032, Caen, France

[c] Department of Physical Chemistry, University of Duisburg-Essen, 45117, Essen, Germany

[d] Interdepartmental Research Centre BIOGEST-SITEIA, University of Modena and Reggio Emilia, 42124, Reggio Emilia, Italy

[*] Corresponding author: hossein.haghighi@unimore.it

Abstract

Natural extracts and plant essential oils (EOs) have long been recognized as valid alternatives to synthetic food additives owing to their proved wide-spectrum antimicrobial capacity. The main aim of this study was to characterize the physical, mechanical, water barrier, microstructural and antimicrobial properties of chitosan-gelatin blend films enriched with cinnamon, citronella, pink clove, nutmeg and thyme EOs. The film microstructure determined by scanning electron microscopy, showed that all active films had heterogeneous surface: in particular, films including cinnamon, nutmeg and thyme EOs showed remarkable pores on the surface. The possible interaction of chitosan-gelatin blend film with incorporated EOs was investigated using Fourier-transform infrared (FT-IR) spectroscopy. Presence of new bands and changes in the FT-IR spectra confirmed intermolecular interactions between the chitosan-gelatin matrix and the EOs. The antimicrobial activity of films was determined using the disk diffusion assay. Active films inhibited the growth of four major food bacterial pathogens including *Campylobacter jejuni, Escherichia coli, Listeria monocytogenes* and *Salmonella typhimurium* and, among the tested EOs, thyme was the most effective ($p<0.05$). The active films can be considered as effective barriers against UV light. The incorporation of EOs to the chitosan-gelatin film increased thickness, moisture content, water vapor

permeability, b* and ΔE* values ($p<0.05$) while it decreased L* value, light transparency and opacity ($p<0.05$). Overall, the characterization of functional properties revealed that chitosan-gelatin films incorporated with EOs could be used as environmentally friendly active food packaging with antimicrobial properties and potential to extend the shelf-life of food products.

Keywords: Bio-Based Active Packaging; Chitosan-Gelatin Blend; Essential Oil; Scanning Electron Microscopy (SEM); Fourier-Transform Infrared Spectroscopy (FT-IR)

1. Introduction

Environmental concerns as well as consumer demand for natural, minimally processed, preservative-free and high-quality food, have raised the attention of food packaging industries on the development of bio-based films enriched with natural compounds. Bio-based films have been considered as attractive alternatives to plastic packaging due to their excellent biodegradability, moreover, they can be blended with active compounds such as antimicrobial agents to protect food against microbial deterioration and to extend the shelf life of food products (De Leo et al., 2018; Shen & Kamdem, 2015).

Among biopolymers, chitosan (CS) and gelatin (GL) have shown outstanding film forming property, non-toxicity, biocompatibility, biodegradability, stability and commercial availability. The CS is a linear polysaccharide, commercially obtainable from deacetylation of chitin. This polycationic biopolymer is soluble in solutions with pH below 6.5 due to the protonation of the amino group (Bonilla, Poloni, Lourenço, & Sobral, 2018). The positively charged amino group of CS interacts with negatively charged microbial cell membranes leading to the leakage of proteinaceous and other intracellular constituents of the microorganisms (Bonilla & Sobral, 2016). Owing to the intrinsic antimicrobial property, chitosan has attracted considerable commercial interest from food packaging companies as a natural alternative to synthetic plastics.

GL is a natural water-soluble protein, obtainable from the partial hydrolysis of collagen. It has a unique amino acid sequence with high contents of proline, glycine and hydroxyproline, which help in the formation of a flexible film with excellent barrier properties to gases, volatile compounds, oils and UV light (Wu, Sun, Guo, Ge, & Zhang, 2017; Figueroa-Lopez, Andrade-

Mahecha, & Torres-Vargas, 2018). Previous studies showed that CS and GL have good barrier to gases such as CO_2 and O_2. However, their use is currently limited due to weak mechanical and water barrier properties. Since CS and GL are hydrophilic biopolymers with good affinity and compatibility, blending CS and GL (CS-GL) to form a composite film may improve mechanical and water barrier response compared to single component films. This is due to the ability to associate through electrostatic interaction between the negatively charged carboxyl group of GL and the positively charged amino group of CS at appropriate pH conditions, and strong hydrogen bond formation (Bonilla et al., 2018; Haghighi et al., 2019). Therefore, blending could combine the advantages of these two biopolymers as well as minimize their disadvantages (Hosseini, Rezaei, Zandi, & Ghavi, 2013; Wang, Qian, & Ding, 2018).

Natural extracts and plant EOs are secondary metabolites of plants that are complex mixtures of low molecular weight compounds. EOs have long been recognized as valid alternatives to synthetic food additive owing to their proved wide-spectrum antimicrobial capacity. Antimicrobial activity of EOs is due to the presence of mono- and sesquiterpenes, mono- and sesquiterpene hydrocarbons and phenolic compounds. These components interact with polysaccharides, fatty acids and phospholipids of bacterial membranes and cause cell death due to the loss of ions and cellular contents (Burt, 2004).

Combination of CS and GL bio-based films with EOs to create bio-based active films is one of the promising strategies that is employed by the food industries to reduce the use of chemical additives (Jamróz, Juszczak, & Kucharek, 2018). The incorporation of EOs into the films instead of applying them directly on foods is an alternative to extend the shelf life of the food and to achieve the desired goal with lower oil concentrations, thus limiting strong aroma and possible changes in the organoleptic properties of the food (Salgado, López-Caballero, Gómez-Guillén, Mauri, & Montero, 2013). In many cases, the active compounds are released slowly onto the food surface from the active films, which act as an active compound reservoir for an extended period. Furthermore, owing to their hydrophobic nature, EOs could improve the water barrier properties of hydrophilic biopolymers such as CS and GL. In this study,

cinnamon (*Cinnamomum zeylanicum*), citronella (*Cymbopogon nardus*), pink clove (*Eugenia caryphyllata*), nutmeg (*Myristica fragrans*) and thyme (*Thymus vulgaris*) were selected for incorporation into CS-GL blend films due to their sensory acceptability and compatibility with food and for their proved antimicrobial properties (Figueroa-Lopez et al., 2018; Ojagh, Rezaei, Razavi, & Hosseini, 2010; Peng & Li, 2014; Shen & Kamdem, 2015; Wu, Sun, Guo, Ge, & Zhang, 2017). Due to the natural origin of EOs, the majority of them have been considered as GRAS by the US Food and Drug Administration (FDA, 2013). Upon addition of EOs into the films, it is also important to evaluate their effects on microstructure, optical properties, mechanical strength, water vapor permeability, moisture content and solubility of the resulting film. However, literature concerning the effects of these EOs on the functional properties of CS-GL blend film is not available. Therefore, the purpose of the present work was to characterize CS-GL films enriched with different EOs including cinnamon, citronella, pink clove, nutmeg and thyme to evaluate some physical, optical, mechanical, water barrier and microstructural properties for potential applications as active food packaging. Moreover, their antimicrobial activity against four common food bacterial pathogens including *Campylobacter jejuni*, *Escherichia coli*, *Listeria monocytogenes* and *Salmonella typhimurium,* was investigated.

2. Material and methods

2.1 Materials and reagents

Chitosan (CS) with a molecular weight of 100-300 kDa was obtained from Acros Organics™ (China). Gelatin (GL) with bloom 128°-192° was purchased from AppliChem GmbH (Darmstadt, Germany). Glycerol (≥ 99.5%) was purchased from Merck (Darmstadt, Germany). Acetic acid (≥ 99.5%) was obtained from Brenntag S.p.A (Milan, Italy). Five types of commercial EOs including cinnamon, citronella, pink clove, nutmeg and thyme were purchased from Solime S.r.l (Cavriago, Reggio Emilia, Italy). Tween 80 was purchased from Sigma-Aldrich (Italy). Brain heart infusion agar (BHIA) was purchased from Biolife (Milan, Italy).

2.2. Preparation of film-forming solutions and films

Preparation of films was adapted from Bonilla & Sobral (2016) with slight modifications. In this study, five different types of films based on a CS-GL blend enriched with EOs (cinnamon, citronella, pink clove, nutmeg and thyme) were analyzed. A film without EO was used as a control. All film forming solutions (FFS) with and without EOs were prepared separately. CS FFS (2%, w/v) was prepared by dissolving CS in an acetic acid solution (1%, v/v) under continuous stirring at 55°C for 30 min. GL FFS (2 %, w/v) was prepared by dissolving GL in distilled water, first being allowed to swell at 7°C for 15 min and then stirred at 55 °C for 30 min. Glycerol (25% w/w of CS or GL) was then added as a plasticizer into both FFS, followed by additional stirring for 30 min. CS-GL blend solution was prepared by mixing CS and GL FFS at 1:1 ratio. Moreover, different types of EOs (1%, v/v) together with Tween 80 (0.2%, v/v EO) were added to FFS, followed by stirring at 55 °C for additional 30 min. All FFS were degasified with a vacuum pump (70 kPa) for 15 min to remove bubbles from the FFS. Films were obtained by casting 20 mL of the FFS into Petri dishes (14.4 cm in diameter) and drying at 25±2 °C overnight in the chemical hood at ambient relative humidity (RH) of 45%.

2.3. Gas Chromatography-Mass Spectrometer (GC-MS) analysis of essential oils volatile profiles

The volatile profiling of the EOs used for incorporation in CS-GL films was carried out by GC–MS analyses using an Agilent (Palo Alto, CA, USA) 6890N GC equipped with a 30 m length, 0.25 mm i.d., 0.25 µm film thickness, fused silica capillary column (Stabilwax®-DA, Restek) coupled with an Agilent 5973 Network mass selective detector. EOs were suitably diluted with acetone and 1 µL was injected into the GC injector port set at 250 °C at 10:1 split ratio. The oven temperature program was as follows: initial temperature 60 °C, then ramp to 200°C at 8°C/min and hold for 1 min, finally ramp to 240 °C at 20 °C/min and hold for 3.5 min. Helium was used as the carrier gas at a flow rate of 1.0 mL/min. Mass spectrometer parameters were as follows: ion source, 230°C; electron energy, 70 eV; multiplier voltage, 1447 V; GC/MS transfer line, 250 °C; and a scan range of 33–650 mass units. Identification of compounds was carried out by comparison with spectra libraries.

2.4. Scanning electron microscopy

Scanning electron microscopy (SEM) of the surface and cross-section of the films were obtained with the use of a scanning electron microscope (FEI, Quanta 200, Oregon, USA). Film samples were fixed on a stainless-steel support with a double side conductive adhesive. The analysis was conducted in low vacuum (0.6 Torr) at an acceleration voltage of 20 kV.

2.5. Attenuated Total Reflection (ATR) / Fourier-Transform Infrared (FT-IR) Spectroscopy

The infrared spectra of different films were obtained using an ATR/FT-IR spectrometer (type Alpha, Bruker Optik GmbH, Ettlingen, Germany). Spectra were collected from two different locations from the top and bottom of the same samples in the 4000-400 cm^{-1} wavenumber range by accumulating 64 scans with a spectral resolution of 4 cm^{-1}.

2.6. Thickness and mechanical properties

Film thickness was measured with a digital micrometer (SAMA Tools measuring Instruments & NTD equipment, Viareggio, Italia) at five different random positions (one at the center and four at the edges). The means of these five separate measurements were recorded.

The tensile stress (TS), elongation at break (EAB) and elastic modulus (EM) were determined using a dynamometer (Z1.0, ZwickRoell, Italy) according to ASTM standard method D882 (ASTM, 2001a). The films with known thickness were cut into rectangular strips (9 x 1.5 cm^2). Initial grip separation and cross-head speed were set at 70 mm and 10 mm/s, respectively. Measurements were repeated 10 times. The software TestXpert® II (V3.31) (ZwickRoell, Ulm, Germany) was used to record the TS curves. TS was calculated by dividing the maximum load to break the film by the cross-sectional area (thickness) of the film and expressed in MPa. EAB was calculated by dividing film elongation at rupture by the initial grip separation expressed in percentage (%). EM was calculated from the initial slope of the stress-strain curve and expressed in MPa. TS and EAB were evaluated for ten samples from each type of film.

2.7. UV barrier, light transmittance, opacity value and color

The barrier properties of films against UV and visible light were determined at the UV (200, 280 and 350 nm) and visible (400, 500, 600, 700 and 800 nm) wavelengths onto square film samples (2 × 2 cm^2) using a Jasco V – 550 UV/Vis spectrophotometer (Jasco Corporation, Tokyo, Japan) as described by Bellelli, Licciardello, Pulvirenti & Fava (2018). The opacity of the films was calculated by Eq. (1):

$$\text{Opacity value} = \frac{-\log T_{600}}{x} \quad (1)$$

where T_{600} is the fractional transmittance at 600 nm and x is the film thickness (mm). The greater opacity value represents the lower transparency of the film. For each film, four readings were taken at different points and average values were determined.

The color of films was measured with a CR-400 Minolta colorimeter (Minolta Camera, Co., Ltd., Osaka, Japan) at room temperature, with D65 illuminant and 10° observer angle. The instrument was calibrated with a white standard (L* = 99.36, a* = -0.12, b* = -0.07) before measurements. Results were expressed as L* (luminosity), a* (red/green) and b* (yellow/blue) parameters. The total color difference (ΔE^*) was calculated using the following Eq. (2):

$$\Delta E^* = \sqrt{[(\Delta L^*)^2 + (\Delta a^*)^2 + (\Delta b^*)^2]} \quad (2)$$

where ΔL^*, Δa^* and Δb^* are the differences between the corresponding color parameter of the samples and that of a standard white plate used as the film background. For each film, five readings were taken at different points and the average values were determined from the top and bottom sides.

2.8. Moisture content and water solubility

Moisture content (MC) of the films was determined by measuring weight loss upon drying to constant weight in an oven at 105 ± 2 °C according to the following Eq. (3):

$$\text{MC (\%)} : \frac{Mw - Md}{Mw} \times 100 \quad (3)$$

Where, Mw and Md are the initial weight and dry weight of the film, respectively.

The initial dry matter content of each film was determined by drying to constant weight in an oven at 105± 2 °C (Wi) and then each film was immersed in 50 mL distilled water at 25 °C.

After 24 h, the film samples (2 × 2 cm^2) were dripped and dried to constant weight at 105± 2 °C (Wf) to determine the weight of dry matter which was not solubilized in water. The measurement of water solubility (WS) was determined according to the following Eq. (4):

$$WS\ (\%): \frac{Wi-Wf}{Wi} \times 100 \quad (4)$$

where, Wi and Wf are initial and final weight of the film, respectively.

2.9. Water vapor transmission rate and water vapor permeability

Water vapor transmission rate (WVTR) of the films was determined gravimetrically in triplicate according to the ASTM E96 method (ASTM, 2001b) with some modifications. Films were sealed on top of glass test cups with an internal diameter of 10 mm and a depth of 55 mm filled with 2 g anhydrous $CaCl_2$ (0% RH). The cups were placed in desiccators containing $BaCl_2$ (75% RH), which were maintained in incubators at 45 °C. WVTR was determined using the weight gain of the cups and was recorded and plotted as a function of time. Cups were weighted daily for 7 days to guarantee the steady state permeation. The slope of the mass gain versus time was obtained by linear regression ($r^2 \geq 0.99$). WVTR (g /day m^2) and WVP (g mm/kPa day m^2) were calculated according to the following Eqs. (5) and (6):

$$WVTR = \frac{\Delta W}{\Delta t \times A} \quad (5)$$

$$WVP = \frac{WVTR \times L}{\Delta P} \quad (6)$$

where $\Delta W/\Delta t$ is the weight gain as a function of time (g/day), A is the area of the exposed film surface (m^2), L is the mean film thickness (mm) and ΔP is the difference of vapor pressure across the film (kPa).

2.10. In vitro antimicrobial activity

Antibacterial activity test on films was assessed against four typical food bacterial pathogens including *Listeria monocytogenes* (UNIMORE 19115), *Escherichia coli* (UNIMORE 40522), *Salmonella typhimurium* (UNIMORE 14028) and *Campylobacter jejuni* (UNIMORE 33250) using the disk diffusion assay according to (Haghighi et al., 2019). Films (sterilized with UV light) were cut into a disc shape of 22 mm diameter and placed on the surface of BHIA agar plates, which had been previously streaked with 0.1 mL of inocula containing 10^6 CFU/mL of

tested bacteria. The plates were then incubated at 30 °C for 24 h (*C. jejuni* plates were incubated at 37 °C). The diameter of the inhibition zones was measured with a caliper and recorded in millimeters (mm). All tests were performed in triplicates.

2.11. Statistical analysis

The statistical analysis of the data was performed through analysis of variance (ANOVA) using SPSS statistical program (SPSS 20 for Windows, SPSS INC., IBM, New York). The differences between means were evaluated by Tukey's multiple range test ($p<0.05$). The data were expressed as the mean ± SD (standard deviation).

3. Results and discussion

3.1. Composition of the essential oils

The volatile profiles of the tested EOs are shown in Tab. 1, which reports the major compounds with their relative abundance (%). Typical chromatograms for each EO are available in the supplementary material (Appendix A). As it can be inferred, eugenol alone accounted for more than 51% of the total peak area of cinnamon EO, while 14 other components contributed from 1 to 6.7% to the total peak area, with β-caryophyllene and benzyl benzoate prevailing, followed by acetyleugenol and linalool, among the most represented. Some differences between our results and other studies were observed, as reported by Wang et al. (2018), cinnamaldehyde was the most representative components of cinnamon EO. The other main constituents were eugenol (19.188%), linalool (4.563%), and beta-caryophyllene (4.551%). In fact, the chemical compositions of the EOs may be varied depending on geographical and climate conditions, herbal species, age, ecotypes, geographical origins and method of drying and isolation of the EOs (Khezrian & Shahbazi, 2018).

The volatile profile of citronella was characterized by citronellal, geraniol and β-citronellol, accounting for about 56%, δ-cadinene, citronellyl acetate, elemol and limonene which, together, made another 22.5%, while other 7 compounds added at least 1% each to the total peak area. Similar finding is reported by Chen et al. (2014) who noted that citronella EO was rich in citronellal (26.23%), geraniol (19.75%) and citronellol (12.96%).

Pink clove EO was the simplest among the studied substances, since it was mainly composed of eugenol (96.5% of total peak area), with minor contributions of carvacrol, β-caryophyllene and vanillin.

Nutmeg EO was composed by about 22.7% sabinene, 14.9 and 10.3% α- and β-pinene, respectively, and many other terpenic compounds, 7 representing 3-7% and 7 more ranging from 1 to 3% of total peak area. Our results on chemical profiling of the nutmeg EO was in accordance with Morsy (2016).

Thyme EO was characterized by p-cymene, thymol and carvacrol, which, together, represented almost 80% of the total chromatographic area. Linalool, α-pinene and borneol contributed for another 13%, while β-myrcene, limonene, β-caryophyllene, camphene and 1,8-cineol accounted for about 1% each. Jouki, Yazdia, Mortazavia, Koocheki, & Khazaei (2014) also reported that thymol (46.42%), p-cymene (22.31%) and carvacrol (12.42%) were the most representative components of thyme EO.

3.2. Microstructure

The surface and cross-section images of CS-GL film (control) and CS-GL film enriched with different EOs (active films) are presented in Fig. 1 and Fig. 2, respectively. The microstructure or internal morphological structures of the film depend on the interactions between film components which directly affect the final physical, optical, mechanical and barrier properties. The surface of control films was smooth and homogenous and did not show pores or cracks (Fig. 1a) indicating the formation of an ordered matrix. Active films showed heterogenous surface that resulted from oil droplets after drying. Both CS and GL have a hydrophilic nature. The incorporation of EO in the FFS is usually carried out by emulsification of the aqueous solution containing the polymer; when the film is dried, droplets of lipid remain embedded into the polymer matrix (Siracusa et al., 2018), as observed in the surface of films incorporated with citronella, pink clove and thyme EOs (Fig. 1b, d, and f). Furthermore, cinnamon and nutmeg films showed remarkable pores on the surface (Fig. 1b and e). The presence of pores might be attributed to the high volatility of these EOs during the drying process (Yao, Ding, Shao, Peng, & Huang, 2017).

A compact and continuous structure without phase separation can be observed in the cross-section of the control film (Fig. 2a) indicating high compatibility among CS and GL to form a blend. The cross-section of active films showed discontinuities and heterogenous structure indicating the occurrence of oil droplets. Moreover, irregular structures with the presence of air bubbles in active films were observed (Fig. 2b, c, d, e, and f). Bonilla et al. (2018) also reported that CS-GL blend film containing eugenol and ginger EOs had uncompact texture with sponge-like structure due to the uneven dispersion of EOs with hydrophobic nature from the aqueous phase during the film drying process.

3.3. Attenuated Total Reflection (ATR) / Fourier-Transform Infrared (FT-IR) Spectroscopy

ATR/FT-IR spectroscopy was performed to characterize the structural and spectroscopic changes due to the incorporation of the EOs into the CS-GL film matrix by measuring the absorbance in the wavenumber range of 4000-400 cm^{-1} at a resolution of 4 cm^{-1}. The FT-IR spectra of control and active films are shown in Fig. 3. The control film spectrum showed the characteristic band at 1636 cm^{-1} (amide-I) due to the ν(C=O) stretching vibration. A strong peak at 1636 cm^{-1} may be taken as evidence of the presence of a significant amount of β-sheet secondary structures of GL in CS-GL film (Haghighi et al., 2019). The peak at 1545 cm^{-1} (amide-II) corresponds to a combination band of the ν(C–N) stretching and δ(N-H) bending vibrations and the weak band at about 1245 cm^{-1} (amide III) has been assigned to another coupled vibration of the −CONH- functionality (Bonilla & Sobral, 2016). The broad absorption band between about 3600 and 3200 cm^{-1} corresponds to ν(O-H) and ν(N-H) stretching vibrations of hydrogen-bonded O-H and N-H functionalities. The band doublet at 2927/2874 cm^{-1} can be assigned to antisymmetric and symmetric $\nu_{as}(CH_3/CH_2)$/$\nu_s(CH_3/CH_2)$ stretching vibrations of CH_3 and CH_2 functionalities. The peaks at 849, 898, 995, 1030, 1150 cm^{-1} can be assigned to saccharide structures of the CS biopolymer in the CS-GL blend film network (Shen & Kamdem, 2015).

The ATR/FT-IR spectra of the active films showed partly characteristic additional bands of the incorporated EOs. It has to be mentioned, however, that due to the low amounts of

admixed EOs, only the most intense absorptions of specific functionalities are observable in the spectra. In Fig. 3 the spectra have been arranged (from top to bottom) in the order of increasing ν(C=O) bands in the wavenumber range 1720-1740 cm^{-1} that can be assigned to ester, aldehyde or ketone functionalities of the EO admixtures. Thus, pink clove and thyme do not show these bands. However, while the spectrum of thyme is - with the exception of weak additional bands in the 2800-3000 cm^{-1} range due to aliphatic functionalities - very similar to the control spectrum, the spectrum of pink clove shows a very characteristic additional peak at 1515 cm^{-1} that belongs to the aromatic ring vibration of the main constituent (eugenol) of pink clove. The CS-GL-Citronella film showed a small new peak at 1733 cm^{-1} and slight changes in the ν(CH) absorption range originating from ester and aldehyde functionalities and aliphatic structures, respectively, of the citronella admixture. The ATR/FT-IR spectra of CS-GL-Cinnamon film showed new peaks in the aliphatic ν(CH) absorption range, at 1743 cm^{-1}, and a significant shoulder at 1515 cm^{-1}, due to aliphatic functionalities, ester and the aromatic structure of linalool, and eugenol components, respectively. The largest changes in the ν(CH) and ν(C=O) absorption ranges are reflected in the CS-GL-Nutmeg film. These changes can be traced back to a major component of nutmeg, trimyristin, a saturated fat which is the triglyceride of myristic acid.

Several of the admixed EOs contain alcoholic OH functionalities but their signatures are too weak and buried in the high-wavenumber wing of the intense, broad ν(NH) band of the CS-GL film. Nevertheless, it can be assumed that the admixed C=O and OH functionalities of the EOs contribute to intermolecular interactions with the hydroxyl and amino groups of the CS-GL film network.

3.4. Thickness

The thickness values for control and active films are reported in Tab. 2. Thickness ranged from 21.66 µm to 33.41 µm: the control film had the lowest value ($p<0.05$), while incorporation of EOs into the CS-GL film increased the thickness ($p<0.05$). Bearing in mind that all films were prepared by casting the same amount of FFS on Petri dishes with the same surface, the difference in thickness might be explained by the different composition of

FFS. Indeed, the addition of low molecular weight EOs into the FFS resulted in disrupting and restructuring of intermolecular interactions between CS and GL, increasing free volumes and the mobility of macromolecules, as it was confirmed by SEM images. Moreover, different chemical compounds present in EOs (Tab. 1) may enhance the spatial distance within the film matrix which lead to thicker films (Khezrian & Shahbazi, 2018). A similar effect of EO on film thickness was reported by Ojagh et al. (2010). In contrast, Siracusa et al. (2018) found that addition of citral EO to pectin and sodium alginate films significantly reduced thickness. This might be due to an increase in homogeneity and to the creation of a well-organized and dense network upon addition of citral EO, but also to the extended drying time required.

3.5. Mechanical properties

The tensile strength (TS), percent elongation at break (EAB%) and elastic modulus (EM) are the most common mechanical parameters for food packaging applications (Acevedo-Fani, Salvia-Trujillo, Rojas-Graü, & Martín-Belloso, 2015). A bio-based film must be resistant to the normal stress that occurs in the application, shipping and handling to maintain the integrity and properties of foods. The mechanical properties of control and active films are presented in Tab. 2. The TS is the measurement of film strength: the films incorporated with cinnamon and pink clove EOs showed lower TS than the control film ($p<0.05$), whereas, films incorporated with citronella, nutmeg and thyme were as resistant as the control film. Several studies reported that the addition of EO reduced TS by decreasing cohesion forces within the polymers in the film matrix (Acevedo-Fani, Salvia-Trujillo, Rojas-Graü, & Martín-Belloso, 2015). It seems likely that strong polymer-polymer interactions between CS and GL molecules are partially replaced by the weaker polymer-oil interactions in the film matrix. Also, EO as a hydrophobic compound causes heterogenous film network and discontinuous microstructure by rearrangement of biopolymers, leading to a decline in the mechanical resistance as it has been confirmed by SEM images (Atarés & Chiralt, 2016; Kim, Beak, & Song, 2018). In contrast, a different result was reported by Ojagh et al. (2010), who found that the addition of EO to CS films significantly increased the TS value. Authors concluded that the strong interaction between CS and EO determined a cross-linking effect leading to

362 an increase in TS. The TS of packaging film must be more than 3.5 MPa, according to
363 conventional standards (Hosseini, Rezaei, Zandi, & Farahmandghavi, 2015). In this study,
364 the TS value of control and active CS-GL films ranged from 29.54 to 47.72 MPa which is a
365 high value for its application as packaging material.

366 The EAB is related to the film flexibility and stretchability. The EAB values ranged from
367 2.18% to 2.90% indicating that all films were quite brittle. No significant difference was
368 observed in the EAB of control and active films ($p>0.05$). Souza et al. (2017) also found that
369 the incorporation of different EOs and hydroalcoholic extracts into CS film did not induce
370 significant differences in EAB values.

371 The EM stands for the resistance of the film to elastic deformation and this parameter
372 indicates the rigidity or stiffness of the film. A low EM value corresponds to a flexible film
373 while a larger EM value indicates a more rigid material. The cinnamon-added films showed
374 the lowest EM value (1340 MPa) meaning that the CS-GL film lost its stiffness and became
375 more flexible with the addition of cinnamon EO ($p<0.05$). However, films containing citronella,
376 pink clove, nutmeg and thyme EOs showed EM values similar to the control film. Overall, it
377 seems that cinnamon EO acts as plasticizer, since it determines a lower TS and a higher
378 EAB (softer and more extensible film). Nutmeg and thyme seem to act as crosslinkers,
379 slightly increasing TS. However, the effects on mechanical properties, are hardly noticeable
380 and may depend on the low relative amounts of EO in the FFSs.

381 ***3.6. UV barrier, light transmittance and opacity value***

382 UV barrier, light transmittance and opacity value of control and active films are presented in
383 Tab. 3. Active films behave as effective UV barriers, since transmittance value was below
384 10% at 280 nm for these films. The UV barrier property of bio-based films is an important
385 parameter for food packaging applications since it can retard lipid oxidation and preserve the
386 organoleptic properties of the packaged food, thereby prolonging its shelf-life (Ramos,
387 Valdés, Beltrán, & Garrigós, 2016).

388 Active films showed lower transmittance in the visible range (350-800 nm) than the control
389 film indicating that the incorporation of EOs into the film matrix reduced the transparency of

the film. The light barrier property is an important factor for food preservation to avoid photo-oxidation of organic compounds and degradation of vitamins and other pigments (Figueroa-Lopez et al., 2018). The control and CS-GL-Thyme films can be considered as transparent (opacity value: 2.62 and 5.23 respectively) while films containing cinnamon, citronella, pink clove and nutmeg EOs were less transparent. Overall, the transparency of the films decreased with the addition of EOs due to the light scattering of oil droplets (with a different refractive index) in the CS-GL film network which interferes with the transmission of light. Similar results were reported by Bonilla, Poloni, Lourenco & Sobral (2018) and Kim et al. (2018).

3.7. Color

The color values (L*, a* and b*) and total color difference (ΔE*) of control and active films are shown in Tab. 4. The L* value, indicating lightness, decreased upon addition of EOs. This value varied between 98.32 and 95.33, which means that all the films were almost clear. A similar result was reported by (Bonilla & Sobral, 2016).

The a* value, expressing the green-red color component, was negative for all films except for those added with cinnamon and pink clove, which showed a slightly positive a* value (+1.92 and +1.33, respectively) due to the presence of red colored substances in the cinnamon and pink clove EOs.

The b* value measures the blue-yellow color component. This value significantly increased upon addition of EOs ($p<0.05$), as to indicate the gain of a slight yellow color. The CS-GL films incorporated with cinnamon and pink clove showed the highest b* value (7.97 and 6.90, respectively) which, in agreement with the a* value, demonstrate the presence of colored compounds into the extracts.

The total color difference (ΔE^*) measures the overall color change of a test sample compared with a reference color. The ΔE^* value varied from 2.50 in the control film to 8.74 in CS-GL-Cinnamon film. The addition of EOs to the CS-GL film generally increased the ΔE^* value ($p<0.05$). The CS-GL films incorporated with cinnamon and pink clove showed the highest ΔE^* values ($p<0.05$) mainly due to the lower brightness (L*) and to the increase observed in

the colorimetric coordinate a* and b*. Some relation can be found also between the higher ΔE^* and the lowest light transmission values observed in the wavelength range 350-500 nm, which suggest that the compounds present in cinnamon and pink clove EOs absorb in this range, which corresponds to the yellow-red color measured by the a* and b* coordinates. Nevertheless, the color of the developed films can change the overall appearance of the food inside the packaging and affecting customer acceptance (Atarés & Chiralt, 2016).

3.8. Moisture content, water solubility and water vapor permeability

The moisture content (MC), water solubility (WS) and water vapor permeability (WVP) of control and active films are presented in Tab. 5. The control film showed the lowest MC value (15.80%), while the addition of EOs increased the MC value ($p<0.05$). The MC is a parameter related to the total free volume occupied by water molecules in the network of the films. The loose microstructure of active films caused the film matrix to have a relatively high free volume and consequently increased the MC as confirmed by SEM images. Similarly, Abdollahi, Rezaei, & Farzi (2012) reported that the addition of rosemary EO to the CS film increased the MC. Authors concluded that the increase in the MC value might be related to the breakup of the film network, which caused an increasing amount of water molecules between polymer chains. In contrast, Nisar et al. (2018) reported that addition of clove EO to pectin film reduced the MC value due to the hydrophobic properties of the EOs and interaction of oil components with hydroxyl groups of pectin film. This could limit the interaction of hydroxyl groups with water molecules, leading to a reduction of MC.

The WS reflects the water resistance and the biodegradability of films (Zhang, Ma, Critzer, Davidson, & Zhong, 2015). Moreover, the WS can determine the release of antimicrobial substances from the films when placed in contact with the food surface (Abdollahi et al., 2012). Water resistance or insolubility is usually essential for potential application of the bio-based films for food packaging applications especially in humid environments (Nisar et al., 2018). The WS of control film was determined as 23.61 %. Addition of nutmeg EOs to the CS-GL film reduced the WS ($p<0.05$) due to the high hydrophobic nature of nutmeg, while, films incorporated with cinnamon, citronella, pink clove and thyme EOs showed an increase

in WS ($p<0.05$). This might be due to the difference in hygroscopic properties of these EOs by which they attract water molecules and the ability to establish polymer-oil interactions which weaken the CS-GL interactions (Gómez-Estaca, López de Lacey, López-Caballero, Gómez-Guillén, & Montero, 2010; Nisar et al., 2018).

The shelf life of some food products is directly related to the transfer of water between the product and the external environment in which they are introduced. Generally, packaging material should reduce this transfer of water to preserve foods from moisture (de Moraes Crizel et al., 2018; Hosseini, Rezaei, Zandi, & Farahmandghavi, 2016; Kim et al., 2018). Therefore, effective control of moisture transfer is a desirable property for the food packaging industry. The CS-GL films containing cinnamon, citronella, pink clove and thyme had higher WVP values compared to the control film ($p<0.05$). The irregular structures with the presence of air bubbles and oil droplets in these films might lead to a weakening of intermolecular interactions between polymer molecules, resulting in an open structure and increased water vapor transfer across the films and consequently an increase of the WVP value. A similar result was reported by Atarés, Bonilla, & Chiralt (2010) that addition of ginger EO to soy protein isolate increased the WVP. These authors concluded that addition of ginger EO might cause disruption in film network and affect the microstructure properties which is a determining factor in WVP value. In this study, despite the statistical differences, the WVP varied between 0.8 and 1.2 (g mm/kPa day m^2). In practical terms, this means that all films were highly permeable to water vapor.

3.9. In vitro antimicrobial activity

Antimicrobial activity of films was evaluated by the disk diffusion assay. The details of antimicrobial activity of control and active films against *C. jejuni, E. coli*, *L. monocytogenes* and *S. typhimurium* are shown in Tab. 6. The control film did not show an inhibitory effect against any of the tested microorganisms. The absence of inhibitory character could be explained by the limitation of CS diffusion in agar medium or incapability of GL to inhibit bacterial growth as it has been reported by other authors (Leceta, Guerrero, Ibarburu, Dueñas, & De La Caba, 2013), so that only microorganisms in direct contact with the active

sites of CS in the CS-GL film network are inhibited (Haghighi et al., 2019; Yuan, Chen, & Li, 2016). Incorporating EOs into the films revealed an antimicrobial effect. In general, due to the hydrophobic nature of EOs, they can interact with polysaccharides, fatty acids and phospholipids of bacteria cell membranes and make them more permeable, so that leakage of ions and cell contents leads to bacterial cell death (Burt, 2004; Salvia-Trujillo, Rojas-Graü, Soliva-Fortuny & Martín-Belloso, 2015). In this study, all active films inhibited the growth of the tested microorganisms. Thyme EO was the most effective ($p<0.05$). Thyme EO showed inhibition activity which was, for all pathogens excluding *L. monocytogenes*, at least double compared to the other EOs. This might be due to the higher WS of CS-GL-Thyme films compared to the other films (Tab. 5). Moreover, thymol and carvacrol are two main phenolic compounds (monoterpenoids) representing 44.2% of the total chromatographic area in thyme EO (Tab. 1). The high antimicrobial activity of phenolic compounds such as thymol and carvacrol has been attributed to structural and functional damages to the bacterial cytoplasmic membrane and to the inhibition of intracellular metabolic pathways (Cao, Yang, & Song, 2018). It should be noted that thyme EO exerted the highest inhibition against *C. jejuni*, *E. coli* and *S. typhimurium*, while its antimicrobial effectiveness against *L. monocytogenes* was lower and comparable with other EOs. In general, the tested EOs were more effective against *C. jejuni* compared to the other considered microorganisms, showing inhibition haloes from 1.5 to 5-fold wider. The only exception to this observation was represented by nutmeg EO, which showed higher inhibition (comparable with the other EOs) of *E. coli* and *L. monocytogenes* but which, however, yielded the lowest effectiveness, hardly noticeable against *C. jejuni* and *S. typhimurium*.

4. Conclusions

In this study, bio-based CS-GL blend active films enriched with cinnamon, citronella, pink clove, nutmeg and thyme EOs (1%, v/v) were developed and their physical, optical, mechanical, water barrier and microstructural properties were evaluated for active food packaging applications. The FT-IR spectra confirmed intermolecular interactions between functional groups of the EOs with the hydroxyl and amino groups of the CS-GL film network.

The results showed that the incorporation of different EOs could notably improve the UV barrier properties of CS-GL film, however, light transparency was reduced. The developed films, with special regards for those including thyme EO, possessed noticeable antimicrobial activity against common food pathogens. The moisture content and water vapor permeability of CS-GL film increased by EOs incorporation due to the microstructure change and presence of pores on the surface as confirmed by SEM. The results suggest that the CS-GL films enriched with different EOs could be used as environmentally friendly, active food packaging with antimicrobial properties and potential to extend the shelf life of food products.

Declarations of interest

None.

Acknowledgments

This work was supported by the Ministry of Agricultural, Food and Forestry Policies of the Italian Government- DG PIUE Prot. Interno N. 0003549 bando sprechi, 2017-2018.

References

1. Abdollahi, M., Rezaei, M., & Farzi, G. (2012). Improvement of active chitosan film properties with rosemary essential oil for food packaging. *International Journal of Food Science and Technology*, *47*(4), 847–853. https://doi.org/10.1111/j.1365-2621.2011.02917.x
2. Acevedo-Fani, A., Salvia-Trujillo, L., Rojas-Graü, M. A., & Martín-Belloso, O. (2015). Edible films from essential-oil-loaded nanoemulsions: Physicochemical characterization and antimicrobial properties. *Food Hydrocolloids*, *47*, 168–177. https://doi.org/10.1016/j.foodhyd.2015.01.032
3. ASTM. (2001a). Standard test method for tensile properties of thin plastic sheeting. In *Annual books of ASTM standards. Designation D882-01. Philadelphia: ASTM, American Society for Testing Materials.*
4. ASTM. (2001b). Standard test method for water vapor transmission of materials. In *Annual books of ASTM Standards. Designation E 96-01, Philadelphia: ASTM, American Society for Testing Materials*.

5. Atarés, L., Bonilla, J., & Chiralt, A. (2010). Characterization of SPI-based edible films incorporated with cinnamon or ginger essential oils. *Journal of Food Engineering*, *99*, 384–391. https://doi.org/10.1016/j.jfoodeng.2010.03.004
6. Atarés, L., & Chiralt, A. (2016). Essential oils as additives in biodegradable films and coatings for active food packaging. *Trends in Food Science and Technology*, *48*, 51–62. https://doi.org/10.1016/j.tifs.2015.12.001
7. Bellelli, M., Licciardello, F., Pulvirenti, A., & Fava, P. (2018). Properties of poly(vinyl alcohol) films as determined by thermal curing and addition of polyfunctional organic acids. *Food Packaging and Shelf Life*, *18*, 95–100. https://doi.org/10.1016/j.fpsl.2018.10.004
8. Bonilla, J., Poloni, T., Lourenço, R. V., & Sobral, P. J. A. (2018). Antioxidant potential of eugenol and ginger essential oils with gelatin/chitosan films. *Food Bioscience*, *23*, 107–114. https://doi.org/10.1016/j.fbio.2018.03.007
9. Bonilla, J., & Sobral, P. J. A. (2016). Investigation of the physicochemical, antimicrobial and antioxidant properties of gelatin-chitosan edible film mixed with plant ethanolic extracts. *Food Bioscience*, *16*, 17–25. https://doi.org/10.1016/j.fbio.2016.07.003
10. Burt, S. (2004). Essential oils: their antibacterial properties and potential applications in foods—a review. *International Journal of Food Microbiology*, *94 (3)*, 223–253. https://doi.org/10.1016/j.ijfoodmicro.2004.03.022
11. Cao, T. L., Yang, S. Y., & Song, K. B. (2018). Development of burdock root inulin/chitosan blend films containing oregano and thyme essential oils. *International Journal of Molecular Sciences*, *19*(1), 131. https://doi.org/10.3390/ijms19010131
12. Chen, Q., Xu, S., Wu, T., Guo, J., S, S., Zheng, X., & Yu, T. (2014). Effect of citronella essential oil on the inhibition of postharvest *Alternaria alternata* in cherry tomato. Journal of the Science of Food and Agriculture, 94(12), 2441-2447. https://doi.org/10.1002/jsfa.6576
13. De Leo, R., Quartieri, A., Haghighi, H., Gigliano, S., Bedin, E., & Pulvirenti, A. (2018).

Application of pectin-alginate and pectin-alginate-lauroyl arginate ethyl coatings to eliminate Salmonella enteritidis cross contamination in egg shells. *Journal of Food Safety*, 1–9. https://doi.org/10.1111/jfs.12567

14. de Moraes Crizel, T., de Oliveira Rios, A., D. Alves, V., Bandarra, N., Moldão-Martins, M., & Hickmann Flôres, S. (2018). Active food packaging prepared with chitosan and olive pomace. *Food Hydrocolloids*, *74*, 139–150. https://doi.org/10.1016/j.foodhyd.2017.08.007
15. FDA (2013). US Food and Drug Administration, Department of Health And Human Services. Code of Federal Regulations part 182: Substances Generally Recognized as Safe sec. 182.20 Essential oils, oleoresins (solvent-free), and natural extractives (including distillates). CFR-Code of Federal Regulations Title 21, volume 3. https://www.accessdata.fda.gov/scripts/cdrh/cfdocs/cfcfr/cfrsearch.cfm?fr=182.20
16. Figueroa-Lopez, K. J., Andrade-Mahecha, M. M., & Torres-Vargas, O. L. (2018). Development of antimicrobial biocomposite films to preserve the quality of bread. *Molecules*, *23*(1), 212. https://doi.org/10.3390/molecules23010212
17. Gómez-Estaca, J., López de Lacey, A., López-Caballero, M. E., Gómez-Guillén, M. C., & Montero, P. (2010). Biodegradable gelatin-chitosan films incorporated with essential oils as antimicrobial agents for fish preservation. *Food Microbiology*, *27*(7), 889–896. https://doi.org/10.1016/j.fm.2010.05.012
18. Haghighi, H., De Leo, R., Bedin, E., Pfeifer, F., Siesler, H. W., & Pulvirenti, A. (2019). Comparative analysis of blend and bilayer films based on chitosan and gelatin enriched with LAE (lauroyl arginate ethyl) with antimicrobial activity for food packaging applications. *Food Packaging and Shelf Life*, *19*, 31–39. https://doi.org/10.1016/j.fpsl.2018.11.015
19. Hosseini, S. F., Rezaei, M., Zandi, M., & Farahmandghavi, F. (2015). Fabrication of bio-nanocomposite films based on fish gelatin reinforced with chitosan nanoparticles. *Food Hydrocolloids*, *44*, 172–182. https://doi.org/10.1016/j.foodhyd.2014.09.004
20. Hosseini, S. F., Rezaei, M., Zandi, M., & Farahmandghavi, F. (2016). Development of

586 bioactive fish gelatin/chitosan nanoparticles composite films with antimicrobial
587 properties. *Food Chemistry*, *194*, 1266–1274.
588 https://doi.org/10.1016/j.foodchem.2015.09.004
589 21. Hosseini, S. F., Rezaei, M., Zandi, M., & Ghavi, F. F. (2013). Preparation and
590 functional properties of fish gelatin-chitosan blend edible films. *Food Chemistry*,
591 *136*(3–4), 1490–1495. https://doi.org/10.1016/j.foodchem.2012.09.081
592 22. Jamróz, E., Juszczak, L., & Kucharek, M. (2018). Investigation of the physical
593 properties, antioxidant and antimicrobial activity of ternary potato starch-furcellaran-
594 gelatin films incorporated with lavender essential oil. *International Journal of*
595 *Biological Macromolecules*, *114*, 1094–1101.
596 https://doi.org/10.1016/j.ijbiomac.2018.04.014
597 23. Jouki, M., Yazdia, F. T., Mortazavi, S. A., Koocheki, A., & Khazaei, N. (2014). Effect
598 of quince seed mucilage edible films incorporated with oregano or thyme essential oil
599 on shelf life extension of refrigerated rainbow trout fillets. *International Journal of*
600 *Food Microbiology, 174*, 88-97. https://doi.org/10.1016/j.ijfoodmicro.2014.01.001
601 24. Khezrian, A., & Shahbazi, Y. (2018). Application of nanocompostie chitosan and
602 carboxymethyl cellulose films containing natural preservative compounds in minced
603 camel's meat. *International Journal of Biological Macromolecules*, *106*, 1146–1158.
604 https://doi.org/10.1016/j.ijbiomac.2017.08.117
605 25. Kim, H., Beak, S. E., & Song, K. B. (2018). Development of a hagfish skin gelatin film
606 containing cinnamon bark essential oil. *Lwt/Food Science and Technology*, *96*, 583–
607 588. https://doi.org/10.1016/j.lwt.2018.06.016
608 26. Leceta, I., Guerrero, P., Ibarburu, I., Dueñas, M. T., & De La Caba, K. (2013).
609 Characterization and antimicrobial analysis of chitosan-based films. *Journal of Food*
610 *Engineering*, *116*(4), 889–899. https://doi.org/10.1016/j.jfoodeng.2013.01.022
611 27. Morsy, N. F. S. (2016). A comprtive study of nutmeg (Myristica fragrans Houtt.)
612 oleoresins obtained by conventionl and green extraction techniques. *Journal of Foos*
613 *Science and Technology 53*(10), 3770-3777. https://doi.org/10.1007/s13197-016-

2363-0

28. Nisar, T., Wang, Z. C., Yang, X., Tian, Y., Iqbal, M., & Guo, Y. (2018). Characterization of citrus pectin films integrated with clove bud essential oil: Physical, thermal, barrier, antioxidant and antibacterial properties. *International Journal of Biological Macromolecules*, *106*, 670–680. https://doi.org/10.1016/j.ijbiomac.2017.08.068
29. Ojagh, S. M., Rezaei, M., Razavi, S. H., & Hosseini, S. M. H. (2010). Development and evaluation of a novel biodegradable film made from chitosan and cinnamon essential oil with low affinity toward water. *Food Chemistry*, *122*(1), 161–166. https://doi.org/10.1016/j.foodchem.2010.02.033
30. Peng, Y., & Li, Y. (2014). Combined effects of two kinds of essential oils on physical, mechanical and structural properties of chitosan films. *Food Hydrocolloids*, *36*, 287–293. https://doi.org/10.1016/j.foodhyd.2013.10.013
31. Ramos, M., Valdés, A., Beltrán, A., & Garrigós, M. (2016). Gelatin-based films and coatings for food packaging applications. *Coatings*, *6*(4), 41. https://doi.org/10.3390/coatings6040041
32. Salgado, P. R., López-Caballero, M. E., Gómez-Guillén, M. C., Mauri, A. N., & Montero, M. P. (2013). Sunflower protein films incorporated with clove essential oil have potential application for the preservation of fish patties. *Food Hydrocolloids*, *33*(1), 74–84. https://doi.org/10.1016/j.foodhyd.2013.02.008
33. Salvia-Trujillo, L., Rojas-Graü, A., Soliva-Fortuny, R., & Martín-Belloso, O. (2015). Physicochemical characterization and antimicrobial activity of food-grade emulsions and nanoemulsions incorporating essential oils. *Food Hydrocolloids*, *43*, 547–556. https://doi.org/10.1016/j.foodhyd.2014.07.012
34. Shen, Z., & Kamdem, D. P. (2015). Development and characterization of biodegradable chitosan films containing two essential oils. *International Journal of Biological Macromolecules*, *74*, 289–296. https://doi.org/10.1016/j.ijbiomac.2014.11.046

642 35. Siracusa, V., Romani, S., Gigli, M., Mannozzi, C., Cecchini, J., Tylewicz, U., & Lotti,
643 N. (2018). Characterization of active edible films based on citral essential oil, alginate
644 and pectin. *Materials*, *11*(10), 1980. https://doi.org/10.3390/ma11101980
645 36. Souza, V. G. L., Fernando, A. L., Pires, J. R. A., Rodrigues, P. F., Lopes, A. A. S., &
646 Fernandes, F. M. B. (2017). Physical properties of chitosan films incorporated with
647 natural antioxidants. *Industrial Crops and Products*, *107*, 565–572.
648 https://doi.org/10.1016/j.indcrop.2017.04.056
649 37. Wang, H., Qian, J., & Ding, F. (2018). Emerging chitosan-based films for food
650 packaging applications. *Journal of Agricultural and Food Chemistry*, *66*(2), 395–413.
651 https://doi.org/10.1021/acs.jafc.7b04528
652 38. Wang, Y., Zhang, Y., Shi, Y., Pan, X., Lu, Y., & Cao, P. (2018). Antibacterial effects of
653 cinnamon (*Cinnamomum zeylanicum*) bark essential oil on *Porphyromonas gingivalis*.
654 *Microbial Pthogenesis*, *116*, 26–32. https://doi.org/10.1016/j.micpath.2018.01.009
655 39. Wu, J., Sun, X., Guo, X., Ge, S., & Zhang, Q. (2017). Physicochemical properties,
656 antimicrobial activity and oil release of fish gelatin films incorporated with cinnamon
657 essential oil. *Aquaculture and Fisheries*, *2*(4), 185–192.
658 https://doi.org/10.1016/j.aaf.2017.06.004
659 40. Yao, Y., Ding, D., Shao, H., Peng, Q., & Huang, Y. (2017). Antibacterial activity and
660 physical properties of fish gelatin-chitosan edible films supplemented with D-
661 Limonene. *International Journal of Polymer Science*, (*2017),1-9*.
662 https://doi.org/10.1155/2017/1837171
663 41. Yuan, G., Chen, X., & Li, D. (2016). Chitosan films and coatings containing essential
664 oils: The antioxidant and antimicrobial activity, and application in food systems. *Food*
665 *Research International*, *89*, 117–128. https://doi.org/10.1016/j.foodres.2016.10.004
666 42. Zhang, Y., Ma, Q., Critzer, F., Davidson, P. M., & Zhong, Q. (2015). Physical and
667 antibacterial properties of alginate films containing cinnamon bark oil and soybean oil.
668 *LWT - Food Science and Technology*, *64*(1), 423–430.
669 https://doi.org/10.1016/j.lwt.2015.05.008

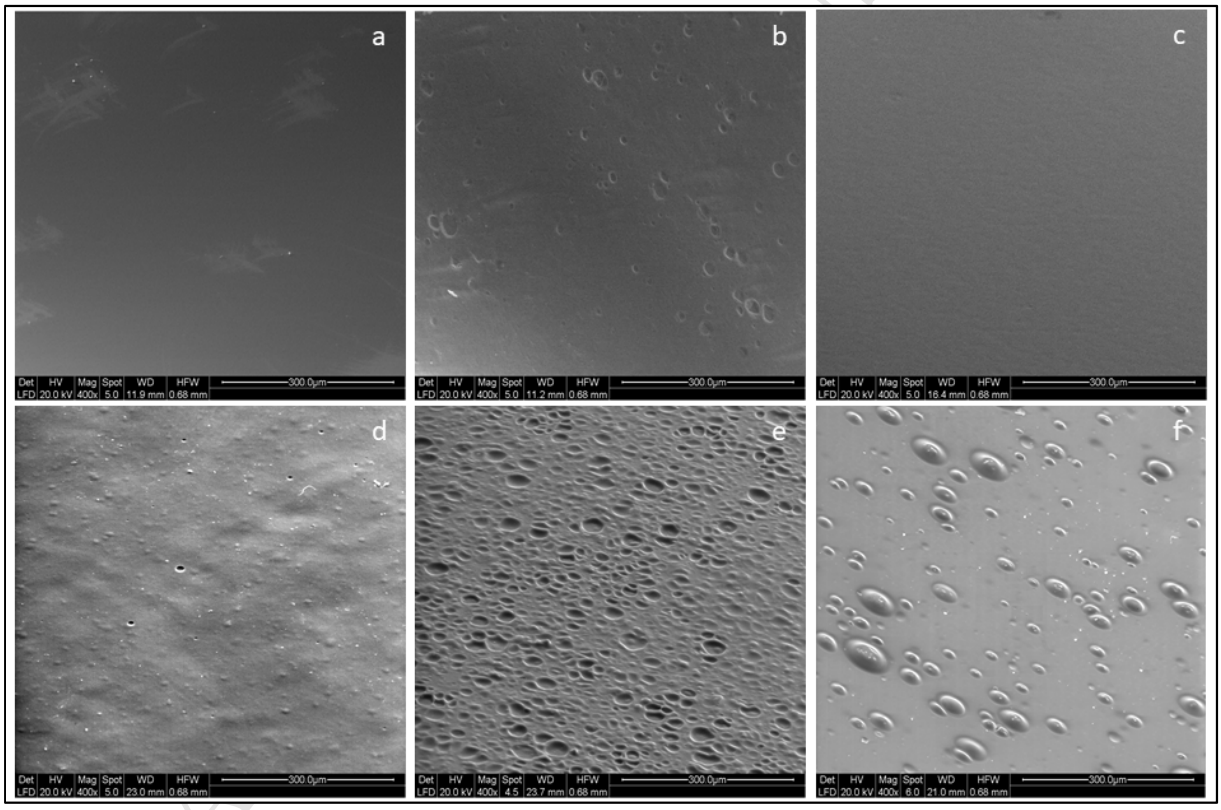

Fig. 1. Scanning electron microscopy (SEM) images of the surface of films. a: Chitosan-Gelatin blend (CS-GL) as a control; b: CS-GL-Cinnamon; c: CS-GL-Citronella; d: CS-GL-Pink Clove; e: CS-GL-Nutmeg; f: CS-GL-Thyme.

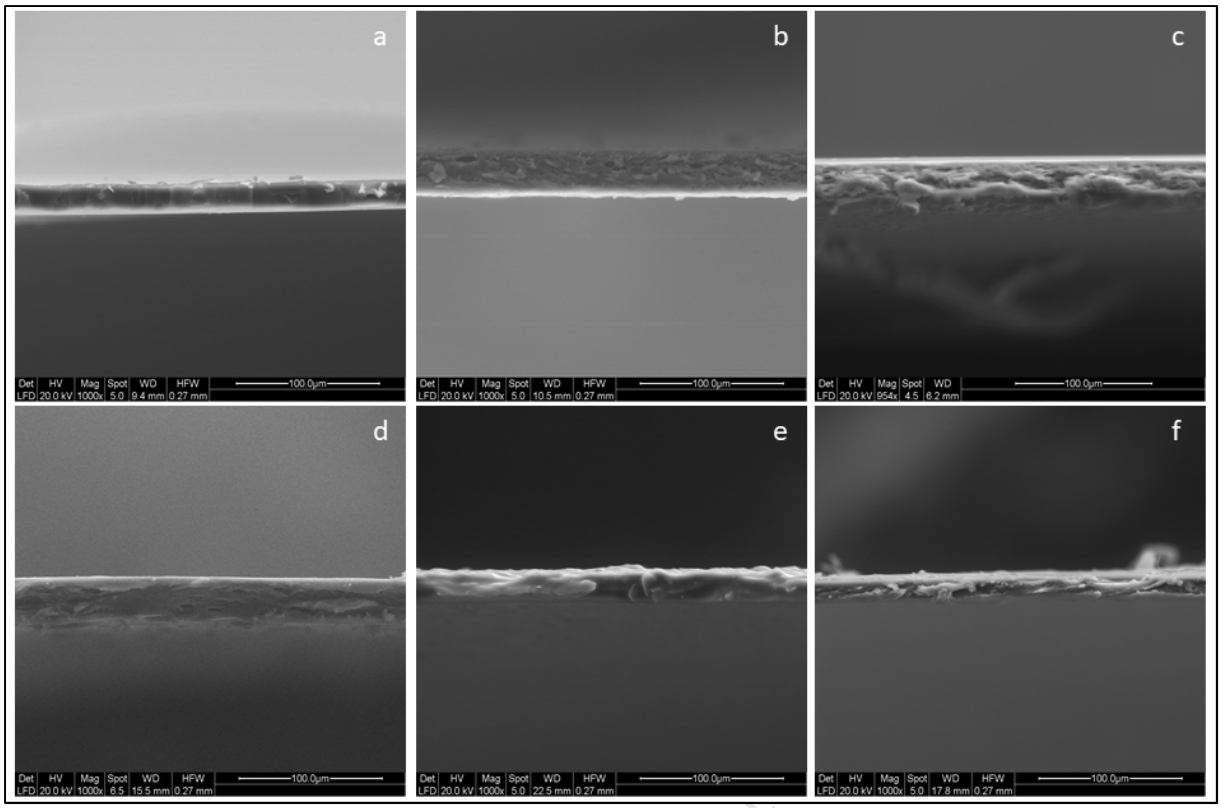

Fig. 2. Scanning electron microscopy (SEM) images on the cross-section of films. a: Chitosan-Gelatin blend (CS-GL) as a control; b: CS-GL-Cinnamon; c: CS-GL-Citronella; d: CS-GL-Pink Clove; e: CS-GL-Nutmeg; f: CS-GL-Thyme.

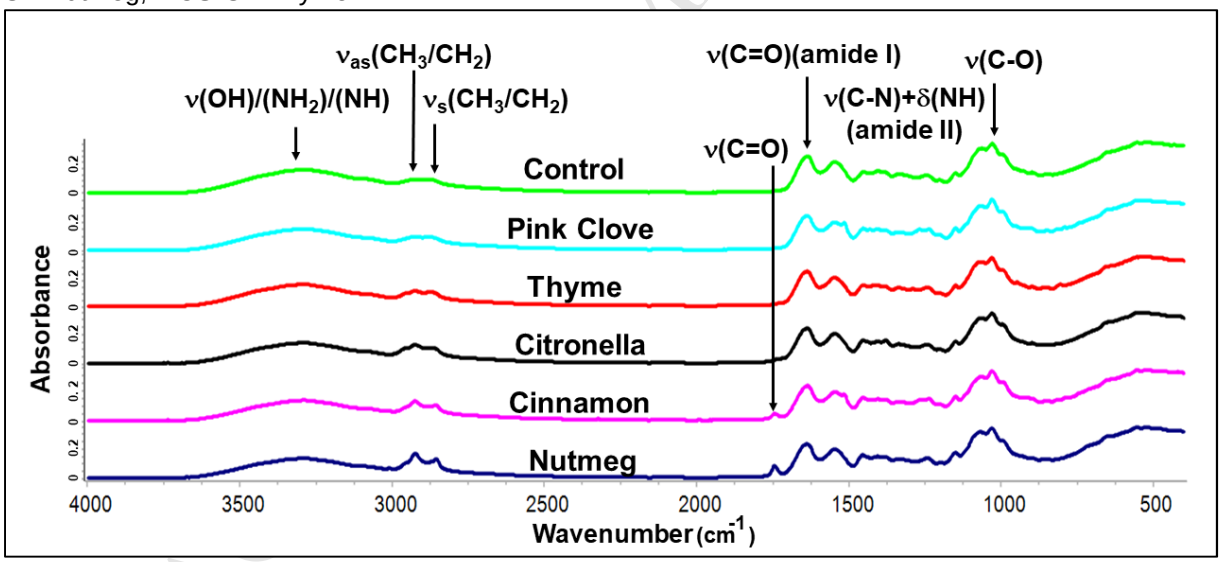

Fig. 3. ATR-FT-IR spectra of films based on a: Chitosan-Gelatin blend (CS-GL) as a control and those enriched with EOs (1%, v/v).

Table 1. Relative volatile composition (main components) of the tested EOs.

NO.	RT* (min)	Compounds name	Cinnamon	Citronella	Pink clove	Nutmeg	Thyme
1	2.23	**α-pinene**	1.8	-	-	**14.9**	4.2
2	2.45	α-fenchene	-	-	-	-	0.2
3	2.52	camphene	0.6	-	-	0.3	1.2
4	2.85	**β-pinene**	0.5	-	-	**10.3**	0.4
5	2.97	**sabinene**	-	-	-	**22.7**	-
6	3.21	δ-3-carene	-	-	-	1.3	-
7	3.30	β-myrcene	-	-	-	2.4	1.3
8	3.37	α-phellandrene	1.1	-	-	1.1	-
9	3.52	α-terpinene	0.2	-	-	3.6	-
10	3.74	limonene	0.6	4.4	-	4.5	1.3
11	3.85	β-phellandrene	1.0	-	-	3.4	-
12	3.85	1,8-cineol	-	-	-	-	0.8
13	4.26	γ-terpinene	-	-	-	5.6	-
14	4.59	**p-cymene**	2.6	-	-	3.0	**34.9**
15	4.72	α-terpinolene	-	-	-	2.1	-
16	7.12	α-cubebene	1.5	-	-	0.2	-
17	7.25	trans thujan-4-ol	-	-	-	0.7	-
18	7.55	**citronellal**	-	**23.9**	-	-	-
19	7.65	α-copaene	-	-	-	0.9	-
20	8.13	camphor	-	-	-	-	0.5
21	8.39	linalool	4.6	1.1	-	0.3	6.6
22	8.51	β-terpineol	-	-	-	0.6	-
23	8.71	1-terpineol	-	-	-	0.3	-
24	8.87	isopulegol	-	3.1	-	-	-
25	8.93	α-fenchyl acetate	-	-	-	0.3	-
26	9.06	β-elemene	-	3.3	-	-	-
27	9.17	β-caryophyllene	6.7	0.1	0.8	1.0	1.2
28	9.31	4-terpineol	0.4	-	-	7.2	-

29	10.07	citronellyl acetate	-	5.4	-	-	-
30	10.16	isoborneol	-	-	-	-	0.4
31	10.21	α-humulene	1.3	0.3	-	-	-
32	10.43	α-amorphene	-	0.4	-	-	-
33	10.59	camphene	-	-	-	0.3	-
34	10.64	α-terpineol	0.6	-	-	0.7	-
35	10.65	borneol	-	-	-	-	2.3
36	10.77	β-cubebene	-	2.5	-	-	-
27	10.96	α-muurolene	-	1.1	-	-	-
38	11.21	citral	-	0.5	-	-	-
39	11.37	δ-cadinene	0.3	8.0	-	0.7	-
40	11.54	**β-citronellol**	-	**13.0**	-	-	-
41	11.99	nerol	-	0.2	-	-	-
42	12.66	**geraniol**	-	**19.2**	-	-	-
43	13.07	safrole	2.9	-	-	1.8	-
44	13.96	allylbenzene	0.2	-	-	-	-
45	14.51	caryophyllene oxide	1.3	-	0.3	-	0.4
46	14.83	methyleugenol	-	-	-	0.7	-
47	15.21	α-amorphene	-	0.8	-	-	-
48	15.43	cinnamaldehyde	2.7	-	-	-	-
49	15.59	elemol	-	4.6	-	-	-
50	16.18	spathulenol	0.2	-	-	-	-
51	16.61	cinnamyl acetate	3.4	-	-	-	-
52	16.69	**eugenol**	**51.2**	2.5	**96.5**	0.3	-
53	16.78	**thymol**	-	-	-	-	**30.2**
54	16.83	muurolol	-	0.6	-	-	-
55	17.12	**carvacrol**	-	-	1.1	-	**14.0**
56	17.28	α-eudesmol	-	0.4	-	-	-
57	17.35	elemicin	-	-	-	2.9	-
58	17.37	α-cadinol	-	1.4	-	-	-
59	17.71	acethyleugenol	4.7	-	-	-	-
60	17.80	**myristicin**	-	-	-	**4.8**	-
61	18.12	cinnamyl alcohol	0.4	-	-	-	-
62	18.68	chavicol	-	-	0.5	-	-
63	20.93	vanillin	-	-	0.8	-	-
64	21.36	benzyl benzoate	6.7	-	-	-	-

* Retention time

The dominant compounds are indicated in bold.

Table 2

Thickness, tensile strength (TS), elongation at break (EAB) and elastic modulus (EM) of the films based on chitosan-gelatin blend (CS-GL) as a control and those enriched with EOs (1%, v/v).

Film sample	Thickness (μm)	TS (MPa)	EAB (%)	EM (MPa)
CS-GL-Control	21.87 ± 1.18^{a}	41.49 ± 4.09^{bc}	2.56 ± 0.09^{ab}	2231 ± 226.13^{bc}
CS-GL-Cinnamon	32.84 ± 1.91^{c}	29.54 ± 2.84^{a}	2.88 ± 0.04^{b}	1340 ± 056.00^{a}
CS-GL-Citronella	30.40 ± 1.59^{c}	36.41 ± 3.15^{ab}	2.18 ± 0.25^{a}	2017 ± 200.89^{b}
CS-GL-Pink clove	32.28 ± 2.16^{c}	32.44 ± 2.96^{a}	2.47 ± 0.28^{ab}	2201 ± 074.36^{b}
CS-GL-Nutmeg	27.40 ± 2.27^{b}	47.72 ± 1.47^{c}	2.52 ± 0.21^{ab}	2374 ± 205.16^{bc}
CS-GL-Thyme	26.67 ± 1.30^{b}	45.18 ± 3.78^{c}	2.56 ± 0.18^{ab}	2661 ± 239.86^{c}

Values are given as mean ± SD (n = 3).

Different letters in the same column indicate significant differences ($p<0.05$).

Table 3

UV and visible light transmittance (T%) and opacity value (600 nm) of the films based on chitosan-gelatin blend (CS-GL) as a control and those enriched with EOs (1%, v/v).

Film sample	Light Transmission (%) at different wavelength (nm)								Opacity value
	200	280	350	400	500	600	700	800	
CS-GL-Control	0.16	38.21	67.12	78.81	85.64	87.62	88.52	88.78	02.62 ± 0.07^{a}
CS-GL-Cinnamon	0.02	0.01	11.36	21.50	25.89	28.42	30.39	31.57	16.67 ± 1.20^{d}
CS-GL-Citronella	0.03	3.05	16.70	22.15	27.84	31.38	34.89	37.64	15.27 ± 2.05^{bc}
CS-GL-Pink clove	0.02	0.01	07.93	26.84	35.24	41.22	44.48	46.60	12.02 ± 0.90^{b}
CS-GL-Nutmeg	0.05	7.53	28.83	37.06	45.04	49.54	53.64	56.29	11.14 ± 0.93^{b}
CS-GL-Thyme	0.09	0.05	57.68	64.45	69.66	72.77	75.07	76.55	05.23 ± 0.47^{a}

Values are given as mean ± SD (n = 3).
Different letters in the same column indicate significant differences ($p<0.05$).

Table 4
Color parameters (L*, a* and b*) and total color difference (ΔE*) of the films based on chitosan-gelatin blend (CS-GL) as a control and those enriched with EOs (1%, v/v).

Film sample	Color parameters			
	L*	**a***	**b***	**ΔE***
CS-GL-Control	98.32 ± 0.34^{c}	-0.52 ± 0.09^{a}	2.16 ± 0.02^{a}	2.50 ± 0.16^{a}
CS-GL-Cinnamon	96.44 ± 1.35^{ab}	+1.33 ± 0.28^{b}	7.97 ± 0.76^{c}	8.74 ± 0.39^{c}
CS-GL-Citronella	97.61 ± 0.24^{bc}	-0.86 ± 0.06^{a}	4.53 ± 0.25^{b}	4.95 ± 0.32^{b}
CS-GL-Pink clove	95.33 ± 0.38^{a}	+1.92 ± 0.86^{b}	6.90 ± 0.35^{c}	8.31 ± 0.56^{c}
CS-GL-Nutmeg	97.55 ± 0.17^{bc}	-0.83 ± 0.11^{a}	4.74 ± 0.50^{b}	5.17 ± 0.56^{b}
CS-GL-Thyme	97.84 ± 0.13^{bc}	-0.59 ± 0.09^{a}	4.30 ± 0.19^{b}	4.63 ± 0.22^{b}

Values are given as mean ± SD (n = 3).
Different letters in the same column indicate significant differences ($p<0.05$).

Table 5
Moisture content (MC), water solubility (WS), water vapor transmission rate (WVTR) and water vapor permeability (WVP) of the films based on chitosan-gelatin blend (CS-GL) as a control and those enriched with EOs (1%, v/v).

Film sample	MC (%)	WS (%)	WVP 75:0% RH (g mm/kP day m^2)
CS-GL-Control	15.80 ± 0.33^{a}	23.61 ± 0.58^{b}	0.8172 ± 0.0027^{a}
CS-GL-Cinnamon	18.71 ± 0.80^{b}	30.24 ± 0.75^{d}	1.1344 ± 0.1298^{bc}
CS-GL-Citronella	19.15 ± 0.44^{b}	26.53 ± 0.53^{c}	1.1396 ± 0.2069^{bc}
CS-GL-Pink clove	23.78 ± 1.81^{c}	29.51 ± 1.40^{d}	1.2460 ± 0.4576^{c}
CS-GL-Nutmeg	17.71 ± 1.39^{ab}	20.36 ± 1.09^{a}	0.8853 ± 0.1237^{ab}
CS-GL-Thyme	18.78 ± 0.97^{b}	31.67 ± 1.71^{d}	1.2851 ± 0.3761^{c}

Values are given as mean ± SD (n = 3).
Different letters in the same column indicate significant differences ($p<0.05$).

Table 6
Inhibition zone diameters of the film disks (22 mm diameter) based chitosan-gelatin blend (CS-GL-Control) as a control and those enriched with EOs (1%, v/v).

Film sample	*C. jejuni*	*E. coli*	*L. monocytogenes*	*S. typhimurium*
CS-GL-Control	N. D.	N. D.	N. D.	N. D.
CS-GL-Cinnamon	5.33 ± 0.94^{bB}	2.66 ± 0.47^{aA}	1.98 ± 0.49^{aA}	1.00 ± 0.14^{aA}
CS-GL-Citronella	4.33 ± 1.88^{abA}	2.83 ± 0.70^{aA}	2.32 ± 0.49^{aA}	2.83 ± 0.70^{aA}
CS-GL-Pink clove	5.33 ± 0.94^{bB}	3.50 ± 0.24^{aAB}	2.42 ± 0.35^{aA}	3.00 ± 0.14^{aA}
CS-GL-Nutmeg	0.44 ± 0.15^{aA}	2.75 ± 0.35^{aC}	2.33 ± 0.47^{aBC}	0.99 ± 0.46^{aAB}
CS-GL-Thyme	11.33 ± 0.94^{cC}	5.66 ± 0.47^{bB}	3.00 ± 0.14^{aA}	6.17 ± 0.70^{bB}

Values are given as mean ± SD (n = 3). N.D means as not detected.
Different lowercase letters in the same column indicate significant differences ($p<0.05$).
Different capital letters in the same row indicate significant differences ($p<0.05$).

Highlights:

- Production of films based on chitosan-gelatin enriched with essential oils
- Determination of the physical, mechanical and barrier properties
- Demonstraion of the interaction between chitosan-gelatin and essential oils
- Improving UV barrier of chitosan-gelatin film by addition of essential oils
- Effectiveness of active films against common food bacterial pathogens

Keywords: Bio-Based Active Packaging; Chitosan-Gelatin Blend; Essential Oil; Scanning Electron Microscopy (SEM); Fourier-Transform Infrared Spectroscopy (FT-IR)